Journal of Innovative Optical Health Sciences
Vol. 2, No. 3 (2009) 289–294

World Scientific
www.worldscientific.com

PRELIMINARY STUDY ON SKIN CANCER DETECTION IN SENCAR MICE USING MUELLER OPTICAL COHERENCE TOMOGRAPHY

MILOŠ TODOROVIĆ
Department of Biomedical Engineering, Texas A&M University
College Station, Texas 77843-3120, USA
milos@tamu.edu

SHULIANG JIAO
Department of Ophthalmology, Keck School of Medicine
University of Southern California, Los Angeles, California 90033, USA
sjiao@usc.edu

GEORGE STOICA
Department of Pathobiology, Texas A&M University
College Station, Texas 77843-5547, USA
gstoica@cvm.tamu.edu

LIHONG V. WANG*
Department of Biomedical Engineering, Texas A&M University
College Station, Texas 77843-3120, USA
lhwang@biomed.wustl.edu

We report on the use of a fiber-based Mueller-matrix optical coherence tomography (OCT) system with continuous source-polarization modulation for *in vivo* imaging of early stages of skin cancer in SENCAR mice. A homemade hand-held probe with integrated optical scanning and beam delivering optics was coupled in the sample arm. The OCT images show the morphological changes in skin resulting from pre-cancerous papilloma formations that are consistent with histology, thus demonstrating the system's potential for early skin cancer detection.

Keywords: Coherence imaging; medical and biological imaging; optical coherence tomography; birefringence; polarization; turbid media.

1. Introduction

Skin cancers are the most common types of cancers occurring in humans. The National Cancer Institute of the US National Institutes of Health had estimated that there would be more than one million new cases of skin cancer diagnosed in 2008 in the United States alone.[1] The deadliest type of skin cancer is melanoma, which forms in melanocytes. Basal cell carcinoma (BCC) develops in the basal layer of the skin, while squamous cell carcinoma

*Corresponding author. Current affiliation: Optical Imaging Laboratory, Department of Biomedical Engineering, Washington University in St. Louis, Campus Box 1097, One Brookings Drive, St. Louis, Missouri 63130-4899, USA.

(SCC) forms in squamous cells on the surface of the skin. Finally, skin cancer that develops in neuroendocrine cells of the skin is called neuroendocrine carcinoma.

Although the overall mortality rate for all skin cancers is lower than for some other types of cancers (breast, colon, prostate, etc.), the high incidence rate has spurred much interest in research of the mechanisms for early detection and treatment. Standard clinical diagnosis of skin cancer relies almost exclusively on the visual examination of tissue followed by pathological determinations of tissue biopsies collected from suspected lesions. Rapid screening of epithelial tissue and early detection of malignant tissue transformations have significant appeal. A method that supplements existing visualization by noninvasively assessing the tissue could prove to be powerful for early detection of epithelial hyperplasia.

Several studies have tackled noninvasive early cancer detection. Prevalent commercially available technologies, such as magnetic resonance imaging[2] and ultrasound,[3] suffer from low resolution and have not proven to be good candidates for early detection of superficial tumors. Stepinac *et al.* have investigated the intraepithelial neoplasiae in Barrett's esophagus using endoscopic fluorescence imaging.[4] The ability of fluorescence imaging to detect the formation of hyperplasiae and neoplasiae on a macroscopic scale has been used to guide optical coherence tomography (OCT) in examination of bladder[5] and oral cavity[6] cancers on a microscopic scale. It has been shown that OCT is capable of detecting pre-cancerous lesions with far better accuracy than fluorescence due to the superior resolution. Garcia-Uribe *et al.* have used spectroscopic oblique-incidence reflectometry to classify skin lesions.[7] Their pilot study achieved a high accuracy in detecting BCC and SCC lesions but their system does not provide visualization of the lesion. Evaluation of superficial pigmented lesions by reflectance-mode confocal microscopy and OCT has been carried out by Yamashita *et al.*[8] Strasswimmer *et al.* have used polarization-sensitive optical coherence tomography (PS-OCT) to investigate the fully developed invasive BCC.[9] They have shown that PS-OCT is capable of delineating the cancer borders using polarization contrast, which can help guide surgeons in the treatment of aggressive skin cancer.

As a branch of PS-OCT, Mueller-matrix OCT[10] provides complete characterization of the polarization properties of a sample by measuring the spatially resolved Mueller-matrix. In this study we used a modified version of the system based on a single light source and a continuously modulated polarization state previously reported by our group.[11] The new system is capable of real-time imaging and, compared to our previous system, possesses improved depth penetration achieved by using a broadband light source with a center wavelength of 1.3 μm. The applicability of the system for early skin cancer detection is demonstrated here by imaging SENCAR mouse skin *in vivo*.

2. Materials and Methods

2.1. *OCT system*

A schematic of the Mueller-matrix OCT system is shown in Fig. 1. Light from a broadband superluminescent diode-based light source (Superlum; center wavelength $\lambda_0 = 1.3\,\mu$m, FWHM bandwidth = 60 nm, output power = 10 mW) is vertically polarized. A polarization modulator (Conoptics; fast axis at 45°) continuously modulates the source-polarization state with a 140 kHz sinusoidal waveform. The incident light beam is split by a nonpolarizing beam splitter and delivered to the reference and sample arms through single-mode optical fibers. A linear polarizer, oriented at −45°, is placed before the entrance of the single-mode optical fiber in the reference arm to control the reference light

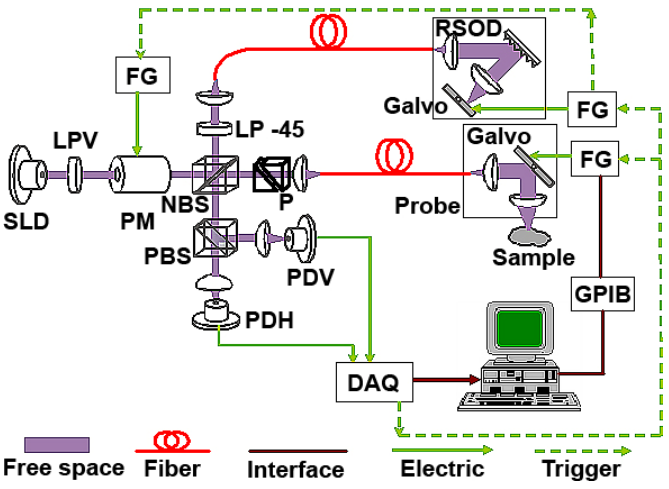

Fig. 1. Schematic of the Mueller-OCT system. DAQ, data acquisition board; FG, function generator; LP −45, −45° linear polarizer; LPV, vertical linear polarizer; NBS, nonpolarizing beam splitter; P, BK7 glass prisms; PBS, polarizing beam splitter; PDH, PDV, photodiodes for horizontal and vertical polarization, respectively; PM, polarization modulator; RSOD, rapid scanning optical delay line; SLD, super-luminescent diode.

polarization state. A grating-based rapid scanning optical delay (RSOD) line[12] is used for longitudinal scanning. A collimating lens, galvanometer scanner, and focusing lens in the sample arm are integrated into a hand-held probe to facilitate *in vivo* imaging. A pair of BK7 prisms is used in the sample arm for dispersion compensation. The combined backreflected sample and reference light is split into horizontal and vertical polarization components by a polarizing beam splitter and detected by two photodiodes. The electrical signal from the photodiodes is filtered, sampled, digitized by a multi-channel data acquisition board (DAQ), and stored on the computer for further processing. The depth resolution of the system is 10 μm in biological tissue, where the index of refraction is assumed to be 1.4. The system is capable of acquiring images consisting of 200 A-scans per frame at a frame rate of 8 fps (frame per second).

Given the band-limited equipment (filters and DAQ), we selected the components of the interference signals at the lowest frequencies to calculate the Jones matrix elements. Those are the terms at the carrier frequency (90 kHz) and the beating frequency (50 kHz). It is important that the polarization modulator not be saturated at any point. The formulae for Jones matrix calculation can be found in our previous publication.[11]

2.2. *Animal studies*

The applicability of the Mueller-OCT to skin cancer imaging was tested using a well-established model of 7,12-dimethylbenz(a)anthracene (DMBA)-induced SCC in SENCAR mice.[13] The SENCAR stock of mice was selectively bred for sensitivity to skin tumor induction by two-stage tumorigenesis using DMBA as the tumor initiator and 12-*O*-tetradecanoylphorbol-13-acetate (TPA) as the promoter. In this study, 30 female SENCAR mice, 7–8 weeks old, were randomly divided into three groups of 10. Each animal was shaved on the dorsal side of the skin. All chemicals were applied topically with a cotton swab. The first group was treated with 0.2 ml of acetone. Second group of mice was treated with TPA (0.2 ml of acetone containing 2 μg of TPA) only. The third group was first treated with DMBA (10 nmol dose dissolved in 0.2 ml of acetone per mouse) once to initiate the tumorigenesis and then, starting one week after initiation, treated with TPA (0.2 ml of acetone containing 2 μg of TPA). The TPA and acetone treatments were repeated once per week up to the termination of the experiment. The experiment was designed to last 20 weeks but had to be terminated after 13 weeks because two mice from group I, one mouse from group II, and four mice from group III died prematurely. Groups I and II served as controls. OCT imaging was performed bi-weekly on one randomly selected animal from each group. Immediately following imaging, the animals were euthanized using the CO_2 method. The excised skin tissue was fixed in a 10% buffered neutral formalin, and the paraffin-embedded tissue was sectioned and stained with hematoxylin and eosin (HE). In addition, the unstained samples were preserved for examination with cross-polarized light microscopy for birefringence detection. The histology slides were examined under an Olympus BH-2 light microscope. All experimental procedures on SENCAR mice were approved by the University Laboratory Animal Care Committee (ULACC) of Texas A&M University and followed the guidelines of the United States National Institutes of Health.[14]

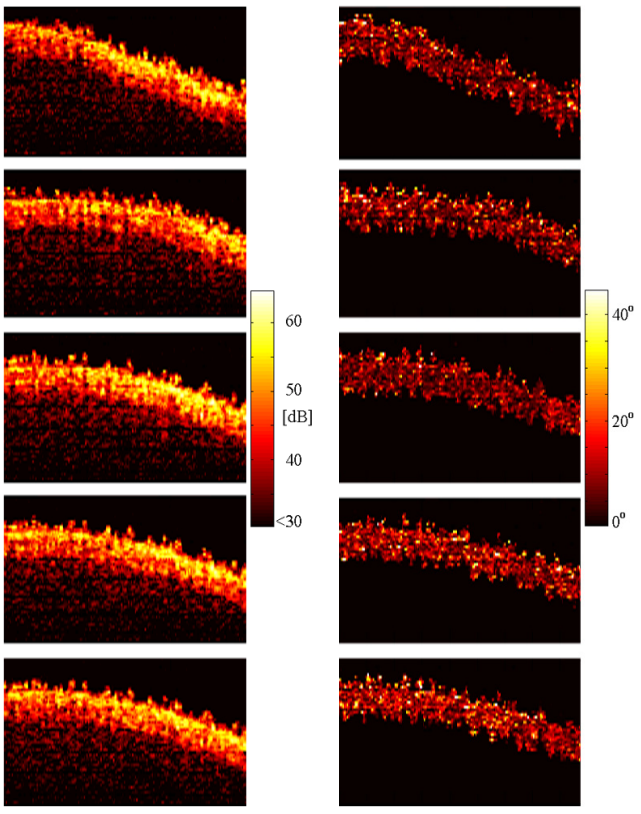

Fig. 2. Intensity (a) and phase retardation (b) images of healthy SENCAR mouse dorsal skin. A set of 5 OCT *in vivo* measurements at the same location proves the repeatability of measurements. Each OCT image is 2 mm wide and 1.2 mm deep.

3. Results and Discussion

The applicability of the Mueller-OCT system for skin cancer detection was tested by imaging the treated dorsal skin of SENCAR mice from all three groups *in vivo*. The experimental results showed no significant difference in skin morphology between the mice in the two control groups (groups I and II). OCT images presented here were acquired 12 weeks after DMBA initiation. OCT images acquired in the first 10 weeks did not show observable differences between the animals from group III and the controls. This observation is in agreement with other SENCAR mouse model studies, where the first registration of papilloma incidence typically occurs at 10–15 weeks after initiation.[13]

Figure 2 presents the OCT images from a set of five measurements taken in succession at the same location on the back of a healthy SENCAR mouse. The purpose of this test is to prove the repeatability of measurements, which is important in this study due to the fact that each animal was imaged only at one time point and immediately sacrificed following imaging. We can see that the retardation images of the five measurements show the same characteristics, which proved the repeatability of measurements.

Figure 3 shows the intensity (a), HE stained histology (b), phase retardation (c), and cross-polarized unstained histology (d) images of healthy SENCAR mouse dorsal skin from group I. Typically, the thickness of the cutis (epidermis and dermis) in healthy mice is in the range of 250–400 μm. In the OCT images in Fig. 3 there is a visible boundary between the dermis and subcutaneous tissue at the depth of approximately 300 μm, which is in agreement with histology. Subcutis is mainly composed of adipose tissue whose backscattered reflectance is low,[15] which explains the low intensity of backreflected light originating from this region. The phase retardation image reveals a low magnitude retardation (up to 50 degrees) indicating weaker birefringence in SENCAR mice skin. The phase retardation is confined within the dermal region, which is consistent with the presence of collagen fibers whose structural organization gives rise to birefringence. In agreement with the

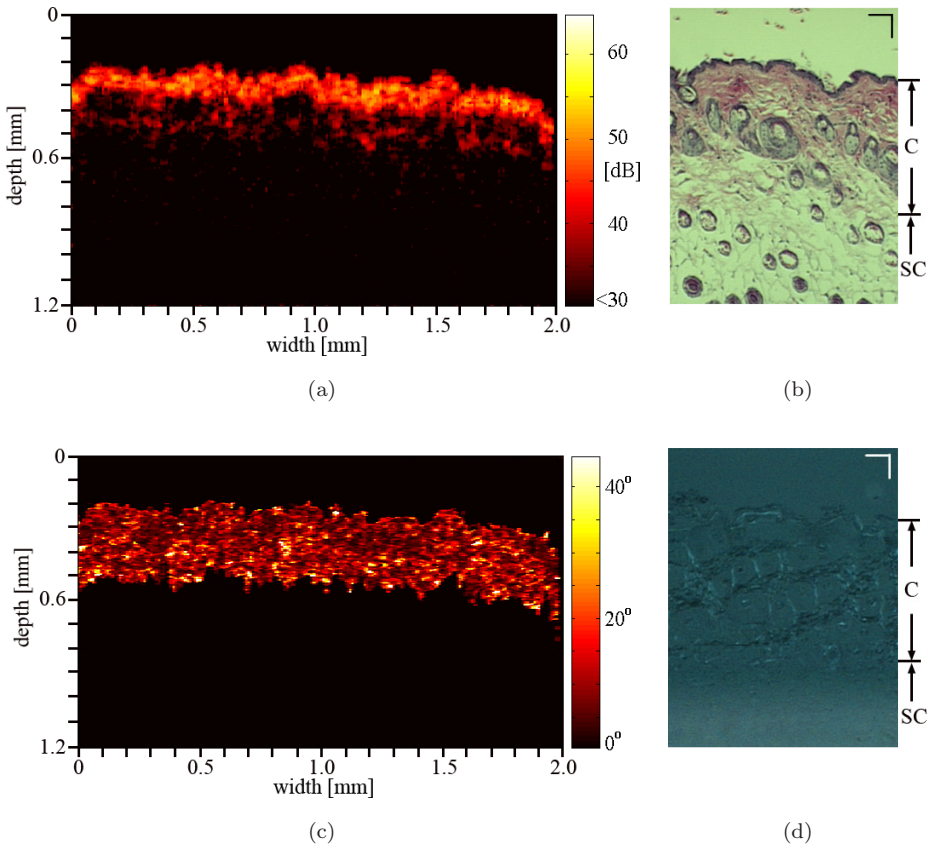

Fig. 3. Intensity (a), HE stained histology (b), phase retardation (c), and cross-polarized unstained histology (d) images of healthy SENCAR mouse dorsal skin. C, cutis; SC, subcutaneous tissue. Bars in histology images represent 100 μm.

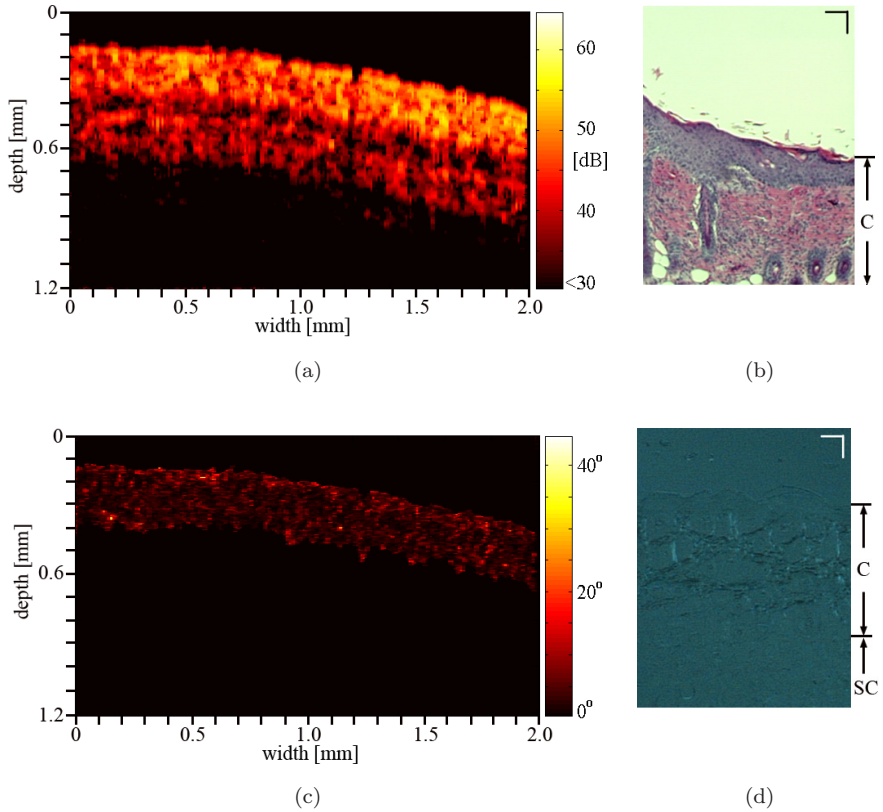

Fig. 4. Intensity (a), HE stained histology (b), phase retardation (c), and cross-polarized unstained histology (d) images of SENCAR mouse dorsal skin with pre-cancerous papilloma formations. C, cutis; SC, subcutaneous tissue. Bars in histology images represent 100 μm.

phase retardation image, the cross-polarized histology image also reveals birefringence.

Figure 4 presents the intensity (a), HE stained histology (b), phase retardation (c), and cross-polarized unstained histology (d) images of SENCAR mouse dorsal skin with pre-cancerous papilloma formations. The intensity image shows a wider cutis (500 μm) due to the proliferation of epidermis and dermis (hyperplasia), which is a typical process in early phases of tumorigenesis. Another important finding is the significant reduction in phase retardation (less than half of that in unaffected skin). The sustained cellular hyperplasia plays a critical role in tumor promotion[16] and is the first indication of potential cancerous formation. The ability to observe these early changes in skin anatomy is important for early cancer detection. The rapid growth of dermis is promoted by the creation of new collagen fibers. These new fibers are immature and not well organized, which reduces the overall birefringence as indicated in the phase retardation image and cross-polarized histology in Figs. 4(c) and 4(d), respectively. The observed reduction in birefringence in the affected region is consistent with the previously published results in the case of invasive BCC.[9]

4. Conclusions

In conclusion, we have presented the use of a high-speed, fiber-based Mueller-matrix OCT system with continuous source-polarization modulation for *in vivo* imaging of skin cancer in a SENCAR mouse model. The system is capable of detecting changes in skin brought about by proliferation of epidermal and dermal tissue as a response to tumor initiation and promotion. The increased depth of cutis coupled with the loss of birefringence, both of which are observed in PS-OCT images, is an indicator of pre-cancerous hyperplasia leading to cancerous SCC.

Acknowledgments

This project was sponsored in part by the Department of the Army (Cooperative Agreement Number: DAMD17-97-2-7016) and the National Institutes of Health (R01 CA092415). The content

of the information presented in this paper does not necessarily reflect the position or the policy of the government or NMTB. No official endorsement should be inferred.

References

1. National Cancer Institute, "Skin cancer," http://www.cancer.gov/cancertopics/types/skin (2008).
2. A. Glaessl, A. G. Schreyer, M. B. Wimmershoff, M. Landthaler, S. Feurbach, U. Hohenleutner, "Laser surgical planning with magnetic resonance imaging-based 3-dimensional reconstructions for intralesional Nd:YAG laser therapy of a venous malformation of the neck," *Arch. Dermatol.* **137**, 1331–1335 (2001).
3. C. C. Harland, S. G. Kale, P. Jackson, P. S. Mortimer, J. C. Bamber, "Differentiation of common benign pigmented skin lesions from melanoma by high-resolution ultrasound," *Br. J. Dermatol.* **137**, 281–289 (2000).
4. T. Stepinac, C. Felley, P. Jornod, N. Lange, T. Gabrecht, C. Fontolliet, P. Grosjean, G. van Melle, H. van den Bergh, P. Monnier, G. Wagnières, G. Dorta, "Endoscopic fluorescence detection of intraepithelial neoplasia in Barrett's esophagus after oral administration of aminolevulinic acid," *Endoscopy* **35**, 663–668 (2003).
5. Y. T. Pan, T. Q. Xie, C. W. Du, S. Bastacky, S. Meyers, M. L. Zeidel, "Enhancing early bladder cancer detection with fluorescence-guided endoscopic optical coherence tomography," *Opt. Lett.* **28**, 2485–2487 (2003).
6. M. Motamedi, R. Johnigan, B. Bell, J. Pasricha, K. Calhoun, "Fluorescence guided optical coherence tomography for early detection of epithelial neoplasia," *Proc. Lasers and Electro-Optics Society 2000 Annual Meeting* **1**, 151 (2000).
7. A. Garcia-Uribe, N. Kehtarnavaz, G. Marquez, V. Prieto, M. Duvic, L. V. Wang, "Skin cancer detection by spectroscopic oblique-incidence reflectometry: Classification and physiological origins," *Appl. Opt.* **43**, 2643–2650 (2004).
8. T. Yamashita, K. Negishi, T. Hariya, N. Kunizawa, K. Ikuta, M. Yanai, S. Wakamatsu, "Intense pulsed light therapy for superficial pigmented lesions evaluated by reflectance-mode confocal microscopy and optical coherence tomography," *J. Invest. Dermatol.* **126**, 2281–2286 (2006).
9. J. Strasswimmer, M. C. Pierce, B. H. Park, V. Neel, J. F. de Boer, "Polarization-sensitive optical coherence tomography of invasive basal cell carcinoma," *J. Biomed. Opt.* **9**, 292–298 (2004).
10. G. Yao, L. V. Wang, "Two-dimensional depth-resolved Mueller matrix characterization of biological tissue by optical coherence tomography," *Opt. Lett.* **24**, 537–539 (1999).
11. S. L. Jiao, M. Todorović, G. Stoica, L. V. Wang, "Fiber-based polarization-sensitive Mueller-matrix optical coherence tomography with continuous source polarization modulation," *Appl. Opt.* **44**, 5463–5467 (2005).
12. G. J. Tearney, B. E. Bouma, J. G. Fujimoto, "High-speed phase- and group-delay scanning with a grating-based phase control delay line," *Opt. Lett.* **22**, 1811–1813 (1997).
13. T. J. Slaga, "SENCAR mouse skin tumorigenesis model versus other strains and stocks of mice," *Environ. Health Persp.* **68**, 27–32 (1986).
14. United States National Institutes of Health, "Guide for the care and use of laboratory animals," US Goverment Printing Office, Washington DC (1985), NIH Publication No. 86–23.
15. M. E. Brezinski, G. J. Tearney, B. E. Bouma, J. A. Izatt, M. R. Hee, E. A. Swanson, J. F. Southern, J. G. Fujimoto, "Optical coherence tomography for optical biopsy: Properties and demonstration of vascular pathology," *Circ. Am. Heart Assoc.* **93**, 1206–1213 (1996).
16. T. J. Slaga, J. DiGiovanni, L. D. Winberg, I. V. Budunova, "Skin carcinogenesis: Characteristics, mechanisms, and prevention," in *Growth Factors and Tumor Promotion: Implications for Risk Assessment*, R. M. McClain, T. J. Slaga, R. LeBoeuf, H. Pitot, Eds., pp. 1–20, Wiley-Liss (1993).